

**ENHANCEMENT OF STRAIN SENSOR SENSITIVITY BY
COMBINATION OF POLARIZATION MAINTAINING FIBER AND
SINGLE MODE FIBER IN SAGNAC LOOP**

ANAS MALIK ABDULRAHMAN

A project report submitted in partial
fulfillment of the requirement for the award of the
Degree of Master of Electrical Engineering

Faculty of Electrical and Electronic Engineering
University Tun Hussein Onn Malaysia

JULY 2019

DEDICATION

I would like to dedicate this thesis to

“ALMIGHTY”

(Who gave me strength, knowledge, patience, and wisdom)

to my beloved “Parents”

(Their love, devotion, cares, sacrifices, and prayers helped me to achieve this dream)



PTTA UTHM
PERPUSTAKAAN TUNKU TUN AMINAH

ACKNOWLEDGEMENT

"Alhamdulillah", all praise to **ALLAH**, the most gracious and the most merciful, for all the strength and will be provided to the author in completing the research. Without "the mercy", the author is just an ordinary person who may not even understand what the research topic is all about.

I would like to express the utmost appreciation and gratitude to the research supervisor, DR. NORAN AZIZAN CHOLAN for his guidance, persistent encouragement and associated aid throughout the research period. His understanding and patience during the tough period is forever appreciated.

I would like also to thank my parents, my family and friends for their kind support, understanding, and encouragement during the completion of my thesis.

I would also like to thank ENGR.AMJAD MUNEIM MOHAMMED for helping me with my study and with the project.

ABSTRACT

Optical fiber-based sensing techniques provide a unique set of sensors which are small, easy to fabricate, lightweight, immune to electromagnetic interference (EMI), high sensitivity, large scale multiplexing, and in most cases inexpensive to manufacture. These advantages are the motivation behind continued researches and development in the field. The introduction, objectives, and the scope of work are presented in the first chapter. A review of the most popular of the optical and non-optical methods that is used to measure the strain is presented in chapter two. The methodology of work, analysis, and the results are presented in chapter three and chapter four, and the conclusion of this project in chapter five. This project investigates the fiber optic sensor technologies that focus on the development of fiber strain sensing element based on a combination of polarization maintaining fiber (PMF) and single mode fiber (SMF) in a Sagnac loop. Four cases are investigated in this work. The first, second, third and fourth cases involve 10 cm PMF, 20 cm PMF, 36 cm PMF + 4 cm SMF and 36 cm PMF + 14 cm SMF respectively as the strain element. Based on the experimental result, strain elements of 10 cm PMF, 20 cm PMF, 36 cm PMF + 4 cm SMF and 36 cm PMF + 14 cm SMF records sensitivities of 6.4 pm/ $\mu\epsilon$, 14.7 pm/ $\mu\epsilon$, 22.8 pm/ $\mu\epsilon$ and 25.3 pm/ $\mu\epsilon$ correspondingly for a range 0-1000 $\mu\epsilon$ at 25 C° temperature. It shows that the strain element of 36 cm PMF + 14 cm SMF possesses the highest sensitivity. In addition to the experimental results, simulation work is also done for comparison. The Sagnac loop model developed with Jones matrices agrees well with the experimental results.

CONTENTS

| | |
|--------------------------------------|------------|
| TITLE | i |
| DEDICATION | ii |
| DEDICATION | iii |
| ACKNOWLEDGEMENT | iv |
| ABSTRACT | v |
| CONTENTS | vi |
| LIST OF FIGURES | ix |
| LIST OF SYMBOLS | xi |
| LIST OF SYMBOLS | xii |
| CHAPTER 1 INTRODUCTION | 1 |
| 1.1 Background | 1 |
| 1.2 Motivation and Problem statement | 2 |
| 1.3 Objective of the project | 4 |
| 1.4 Scope of study | 4 |
| 1.5 Project outline | 4 |
| 1.6 Summary | 6 |
| CHAPTER 2 LITERATURE REVIEW | 7 |
| 2.1 Introduction | 7 |

| | | |
|------------------|--|-----------|
| 2.2 | Non-optic strain sensors | 7 |
| 2.2.1 | The Whittemore gauge | 7 |
| 2.2.2 | Electrical resistance strain gauge | 9 |
| 2.2.3 | Vibrating wire strain gauge | 10 |
| 2.2.4 | Video extensometer | 11 |
| 2.2.5 | Laser speckle strain measurement | 12 |
| 2.3 | Fiber optic sensor technology | 14 |
| 2.3.1 | Advantages of Fiber Optic Sensors | 14 |
| 2.3.2 | Fiber Optic Sensory Systems | 15 |
| 2.3.3 | Sources | 16 |
| 2.3.4 | Detector | 16 |
| 2.3.5 | Sensor Types | 16 |
| 2.4 | Fiber Optics Strain sensors | 18 |
| 2.4.1 | Microbend Sensor method | 18 |
| 2.4.2 | Bragg Grating Sensor | 20 |
| 2.4.3 | Mach-Zehnder Interferometer Sensors | 22 |
| 2.4.4 | Fabry-Perot interferometer sensor | 24 |
| 2.4.5 | Michelson Interferometer Sensors | 25 |
| 2.4.6 | Sagnac Interferometer Sensor | 27 |
| 2.5 | Summary of previous related works | 29 |
| CHAPTER 3 | MEHTODOLOGY | 34 |
| 3.1 | Introduction | 34 |
| 3.2 | Operational framework | 34 |
| 3.3 | Analyzing the Sagnac Loop Using Jones Matrices | 36 |
| 3.4 | Simulation of Sagnac Filter | 38 |

| | | |
|------------------|--|-----------|
| 3.5 | Develop and characterize strain sensor using (PMF) and (SMF) | |
| 39 | | |
| 3.5.1 | Amplified Spontaneous Emission (ASE) | 39 |
| 3.5.2 | Polarization maintaining fiber (PMF) and (SMF) | 40 |
| 3.6 | Experiment setup | 41 |
| 3.7 | Chapter summery | 44 |
| CHAPTER 4 | RESULTS AND ANALYSIS | 45 |
| 4.1 | Introduction | 45 |
| 4.2 | Analyzing and simulate SLF | 45 |
| 4.3 | Strain sensor enhancement | 47 |
| 4.3.1 | The first case (strained 10 cm PMF) | 47 |
| 4.3.2 | The second case (strained 20 cm PMF) | 48 |
| 4.3.3 | The third case (strained 36 cm PMF and 4 cm SMF) | 49 |
| 4.3.4 | The fourth case (strained 36 cm PMF and 14 cm SMF) | |
| 50 | | |
| 4.4 | Summery | 52 |
| CHAPTER 5 | CONCLUSION AND RECOMMENDATION | 53 |
| 5.1 | Conclusion | 53 |
| 5.2 | Recommendation and future work | 54 |
| REFERENCE | | 55 |
| APPENDIX | | 61 |

LIST OF FIGURES

| | | |
|------|---|----|
| 1.1 | Types of Crack (small, large, and multi crack) | 3 |
| 1.2 | project flow | 5 |
| 2.1 | Whittemore gauge[9] | 8 |
| 2.2 | Concrete with metal points on the surface | 8 |
| 2.3 | Electrical resistance strain gauge | 9 |
| 2.4 | Vibrating wire strain gauge[14] | 11 |
| 2.5 | Video extensometer configuration[16] | 11 |
| 2.6 | Principle of speckle generation[18] | 13 |
| 2.7 | Speckle pattern | 14 |
| 2.8 | Optical circuit using a tuneable laser source[21] | 15 |
| 2.9 | Optical circuit using a broadband source | 15 |
| 2.10 | Microbending in multi-mode fiber light traveling close to critical angle | 18 |
| 2.11 | Microbending in multi-mode fiber light ray exceeding critical angle due to microbend[28] | 19 |
| 2.12 | Microbend Sensor configuration[29] | 20 |
| 2.13 | The architecture of fiber bragg grating[30] | 20 |
| 2.14 | Basic operation of MZI[33] | 22 |
| 2.15 | Configuration of various types of MZIs; the methods of using (a) a pair of LPGs, (b) core mismatch, (c) air-hole collapsing of PCF, (d) MMF segment, and (e) small core SMF[34] | 24 |
| 2.16 | (a) Extrinsic FPI sensor made by forming an external air cavity, and (b) intrinsic FPI sensor formed by two reflecting components, R1 and R2, along a fiber[34] | 25 |

| | | |
|------|--|----|
| 2.17 | Michelson Interferometer Sensors[41] | 26 |
| 2.18 | Schematic sensor based on Sagnac interferometer | 27 |
| 2.19 | The setup of Sagnac interferometer combined with a pair of LPG MZI sensor. | 28 |
| 3.1 | The specific Flow chart of project | 35 |
| 3.2 | The structure of Sagnac loop filter | 36 |
| 3.3 | EDFA-UPM-C100 | 40 |
| 3.4 | Schematic diagram of Panda fiber[53] | 41 |
| 3.5 | Single mode fiber | 41 |
| 3.6 | Experiment setup | 42 |
| 3.7 | Case 1 (strained 10 cm PMF) | 43 |
| 3.8 | Case 2 (strained 20 cm PMF) | 43 |
| 3.9 | Case 3 (strained 36 cm PMF and 4 cm SMF) | 43 |
| 3.10 | Case 4 (strained 36 cm PMF and 14 cm SMF) | 44 |
| 4.1 | Spectrum output of SLF using Jones matrices simulation | 46 |
| 4.2 | Spectrum output of SLF using experiment | 46 |
| 4.3 | The output spectrum within different strain levels | 47 |
| 4.4 | Wavelength shifting of the transmission dip versus strain | 48 |
| 4.5 | Wavelength spectra with different strain | 48 |
| 4.6 | Shifting of dips as function of strain | 49 |
| 4.7 | Wavelength dips as function of strain | 50 |
| 4.8 | Output spectrum for strain range 0-850 $\mu\epsilon$ | 50 |
| 4.9 | Shifting of wavelength dips function of strain | 51 |
| 4.10 | Strain sensitivities for the four cases | 52 |

LIST OF SYMBOLS

| | |
|---------------------------|---|
| α | Coefficient of thermal expansion for optical fiber |
| α_{host} | Coefficient of thermal expansion for host material |
| λ | Input wavelength of the source |
| λ_B | Bragg wavelength |
| Λ | Grating pitch |
| ν | Poisson ratio |
| $\Delta\lambda_B$ | Bragg wavelength shift |
| ΔT | Thermal variations |
| ε | Strain variations |
| $\mu\varepsilon$ | Micro-strain |
| $^{\circ}\text{C}$ | Degree Celsius |
| C_1 | Constants of integration on strain in optical fiber |
| E | Young Modulus |
| L | Length |
| m | Meter |
| mm | Millimeter |
| μm | Micro-meter |
| n_{eff} | Effective refractive index of optical fiber |
| $n_{\text{eff}}(\lambda)$ | Effective refractive index based on wavelength of input light |
| n_{core} | Refractive index of the optical fiber core |
| P_{11} | Strain-optic coefficients |
| P_{12} | Strain-optic coefficients |
| P_e | Strain-optic parameter |
| ΔL | Elongation of length |
| PC | Polarization controller |
| M_{PC} | Polarization controller matrix |

LIST OF TABLES

| | | |
|-----|--|----|
| 2.1 | The summary of the related work | 30 |
| 2.5 | Gantt chart plans on semester 1 Master project | 61 |
| 3.5 | Gantt chart plans on semester 2 Master project | 62 |



CHAPTER 1

INTRODUCTION

1.1 Background

Optical fiber sensors have been studied intensely for more than 30 years with their applications developed rapidly in variety of areas in recent years. Initially, most of the fiber sensors remained laboratory-based at the prototype stage and were developed to replace conventional electro-mechanical sensors which are well established, have proven reliabilities and relatively low manufacturing costs, thus fewer commercial successes have been achieved. In recent years, the manufacturing cost of fiber sensors is decreasing and more fiber sensors are implemented for industrial applications. Optical fiber sensors offer important advantages such as electrically passive operation, EMI immunity, high sensitivity, and large-scale multiplexing capability. The promising utilization of optical fiber sensors plays an important role in variety of areas include civil engineering structural monitoring, textile structural composites monitoring, railway, spacecraft, marine, nuclear and medical applications[1].

Optical fiber sensors have been widely used to measure a range of parameters including refractive index, distance, concentration, strain, and humidity. They can be classified in various ways but, often, the measurement scheme is chosen as the main criterion for classification. Optical fiber sensors based on measurement schemes are divided into two broad categories: intensity-based and wavelength based. Wavelength-based sensors measure the physical parameter based on its influence on the wavelength of light. On the other hand, intensity-based sensors, measure parameters based on the

effect of the physical parameter on the intensity of either the reflected or transmitted light[2].

There are many methods used as optical fiber sensors such as: Microbend sensor, Fiber Bragg Grating strain sensor, Fabry-Perot interferometer sensor, Michelson interferometer, and Sagnac loop interferometer sensor[3][4][5][6]. Sagnac loop interferometer is most popular method because of it is simple, high sensitivity, easy to fabricate and suitable for many different fibers. For these advantages, it is used in this project. Sagnac fiber loop consist of a source of light, fiber coupler, a section of optical fiber, and optical oscillator[7].

1.2 Motivation and Problem statement

A lot of civil infrastructure systems, whose functional integrity is vital to the economic growth and well-being, are increasingly vulnerable to man-made and natural hazards such as neglect of maintenance, vehicular overloads, earthquakes, hurricanes, and floods so it costs billions of money losses and thousands of people life. It is true that we cannot control non man-mode like earthquakes and hurricanes, but we can avoid it with minimum losses by detecting before it happen, so reliable health-monitoring systems are pertinent to provide vital information about the safety of civil structures and important roles in securing civil infrastructures' integrity, minimizing the maintenance cost, and maintaining longevity of existing and future structural systems including buildings, bridges, and utility facilities in adverse environment. Meanwhile, monitoring can also provide verification of current design/analysis models in civil engineering practice, and suggest improvement for retrofits and future constructions. Sensors are the most important components of a monitoring system, just like eyes to human being. Successful monitoring depends very much on reliable, easy-to-use, and cost-effective sensor devices.

There are many types of sensor. Unfortunately, conventional electric type sensors suffer from major difficulties, which prevent them from being widely and successfully applied in monitoring civil structures. For instance, they can be easily interfered by

electromagnetic field, which is unavoidable in a modern civil structure with complex functions. Using electrical cables for signal transmission and power supply, which may act as antenna picking up various kinds of noise, and are susceptible to lightning strikes. These cables need to be electrically shielded to mitigate the electromagnetic interference problem, and shielding makes them expensive and heavy. A large number of sensors are required to monitor a civil structure usually of large size, and each of them requires, expensive and cumbersome installation of long electrical cables in need of heavy shielding. Therefore, the cabling is a very labor intensive and costly process. The emerging optical fiber sensor technology has shown great potential for overcoming the difficulties associated with conventional sensors and does not suffer from electromagnetic interference, noise immunity, no High transmission security, no cross-talk, no spark/fire hazards, no short-circuit loading, no High temperature operation, wide bandwidth, light weight, Longer distance signal transmission. Second, the cables of these sensors are optical fibers, which are extremely light in weight. Therefore, many of the cabling problems observed in the conventional sensors do not exist in these optical fibers sensors, which is a huge advantage for their applications in monitoring large-scale civil structures. Moreover, their cost can be competitive to their conventional counterparts, due to the steadily decreasing costs of key optical fiber components in the ever-expanding commercial telecommunication market. Figures 1.1 shows different types of cracks.

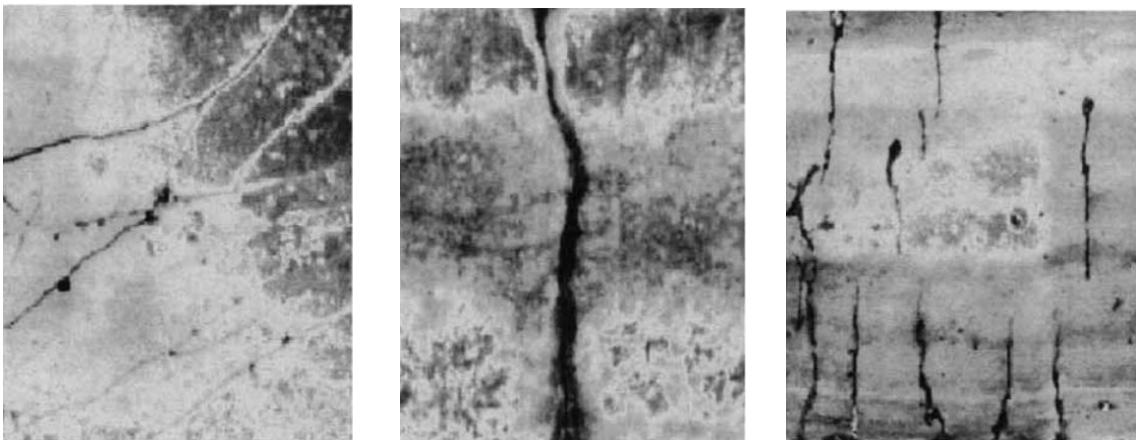


Figure 1. 1: Types of Crack (small, large, and multi crack)

1.3 Objective of the project

The aim of this project is to enhance the strain sensitivity by using low-birefringence polarization maintaining fiber (PMF) (Panda) and single mode fiber (SMF) without the effect of the temperature. This project is conducted to achieve the following objectives:

- 1) To analyze and simulate single sagnac loop interferometer mathematically.
- 2) To test the polarization maintaining fiber (PMF) (panda) based on sagnac loop as strain sensor.
- 3) To enhance the strain sensitivity by combining low-birefringence polarization maintaining fiber (PMF) and single mode fiber (SMF) with different lengths.

1.4 Scope of study

In order to produce a more specialized and specified research and study about the sagnac loop and strain sensitivity, the scope of this research has been limited to the constraints listed below:

- 1) Jones matrix used for mathematical analysis and simulating the single loop fiber (SLF).
- 2) To simulate the output spectrum from the sagnac loop, MATLAB software program used.
- 3) For testing and enhancing the strain sensitivity, Erbium Doped Fiber Amplifier (EDFA), optical spectrum analyzer (OSA), 3-dB coupler, (PMF), and (SMF) are used.

1.5 Project outline

This project contains five chapters as shown in figure 1.2. The current chapter has described a background of optical fiber sensors, the main advantages, what is the reasons of being preferred than other types of sensors, the motivation and problem statement, objectives, scope and dissertation flow. Chapter 2 contains a historical background of

optical and non-optical methods that are used as strain sensors. Also, it contains definitions for the equipment that is used in this research. Chapter 3 is the methodology of this research. Chapter 4 contains the result and the discussion. Chapter 5 is the conclusion of this research.

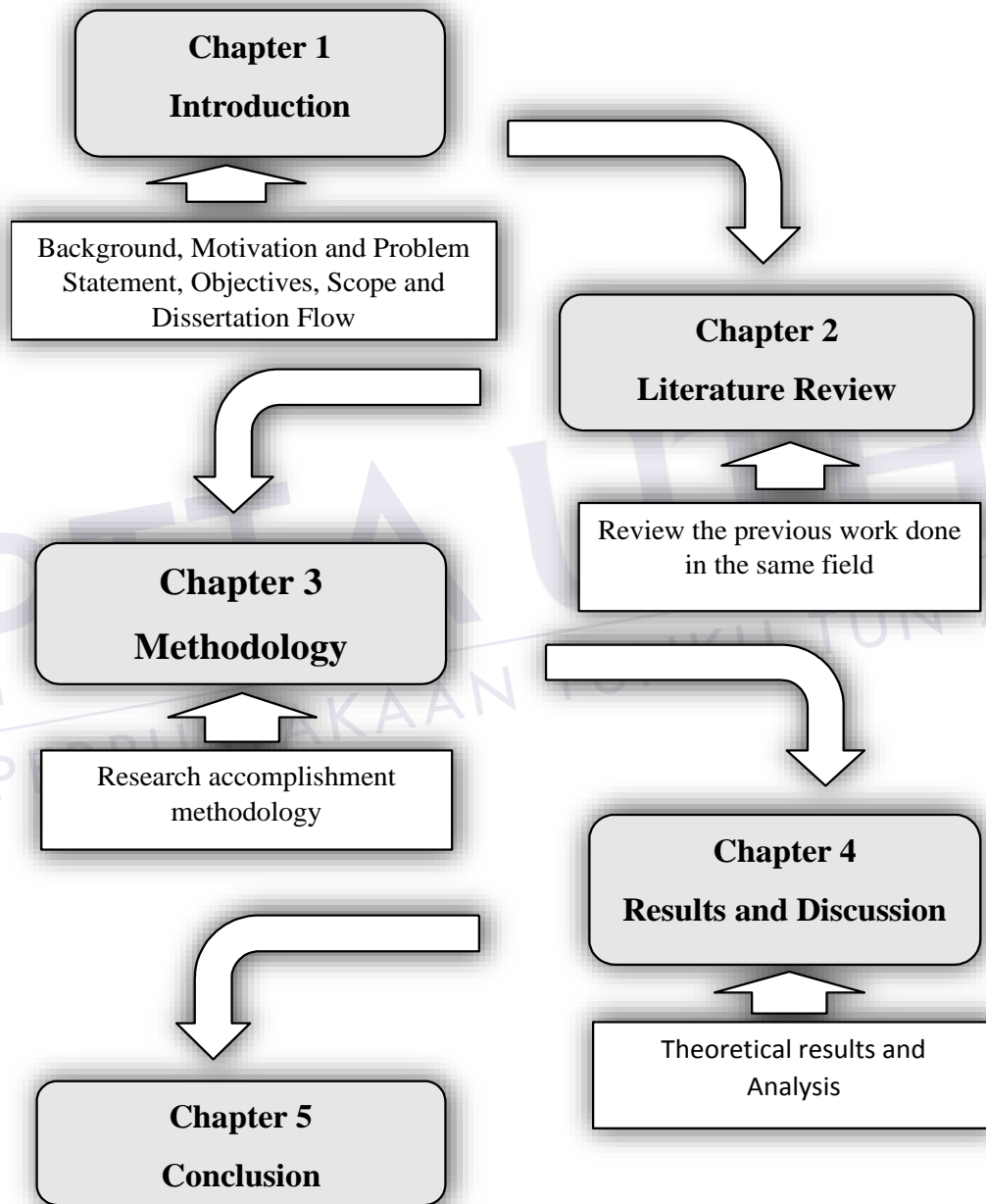


Figure 1.2: project flow

1.6 Summary

In this chapter, introduction to the project has been presented. This include the back ground of the strain sensors and the reason for continue the recaches int his field, motivation, problem statement, objectives, and the scope of this project.



CHAPTER 2

LATIRATURE REVIEW

2.1 Introduction

Literature review is a vital part of the research, it was similar an overall analysis or research on all comparisons of existing project in selected fields. In this part, the details of this project will be explained. The relevant discussion, contradiction, problem or knowledge is explained in this part.

2.2 Non-optic strain sensors

This section, review the common and the most popular non-optic methods which used to test the strain sensitivity.

2.2.1 The Whittemore gauge

The Whittemore gauge as shown in Figure 2.1 is a mechanical strain gauge that has been widely used for measuring surface strain of concrete structures for decades. Before a strain reading can be made, small steel circular buttons with a precision pinhole at the center, called “points”, are bonded on the concrete surface by using epoxy as shown in Figure 2.2. The Whittemore gauge measures the distance between the pinholes of successive pairs of points. Prior to the surface deformation, a set of reference length measurement is made, representing the unstrained positions of the points. Then a second measurement is taken after the surface deformation. The difference between the second

measurement and the reference length is divided by the gauge length 203.2mm (8”), giving the strains on the concrete surface. When a reasonable strain profile is required, tens of points must be bonded onto the concrete surface, which is very time consuming and labor-intensive[8].



Figure 2.1: Whittemore gauge[9]



Figure 2.2: Concrete with metal points on the surface

2.2.2 Electrical resistance strain gauge

Electrical resistance strain gauge is a traditional method used to measure the strain on the surface[10]. It employs the principle that metallic conductors subjected to mechanical strain exhibit a change in their electrical resistance. By converting mechanical strain into an electronic signal, the electrical resistance strain gauge can measure strain to quite high resolution.

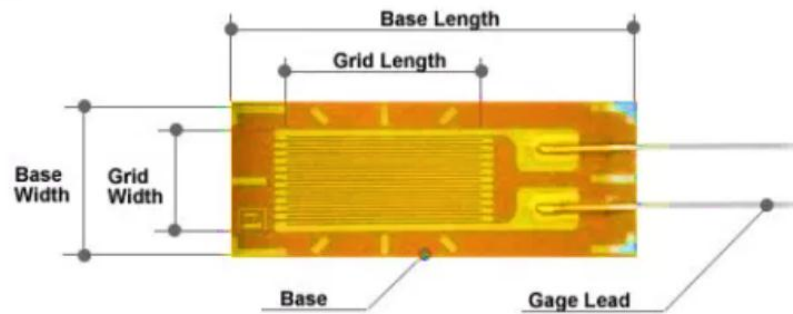


Figure 2.3: Electrical resistance strain gauge

In general, the electrical resistance strain gauge is precise, reliable and easy to use. However, the technique has several disadvantages.

- 1) The technique requires gluing the gauge on the specimen surface. Since the gauge has contact with the specimen surface, it may influence the surface strain and cause measurement error.
- 2) It is difficult to bond the gauge to the rough surface such as concrete.
- 3) Temperature, material properties and the adhesive that bonds the metallic conductors to the surface all affect the detected resistance, and hence can interfere with the accuracy of the strain measurement[11].
- 4) The electrical resistance strain gauge is sensitive to electromagnetic interference (EMI), which could cause measurement error when used in the industrial environment where many types of EMI inducing equipment are present, such as motors or electrical heaters.

- 5) In a harsh environment, the glue may debone and the gauge may break off from the specimen surface, making the measurement impossible.
- 6) In the case of large and suddenly changing surface strain, the gauge may suffer from “creep effect”. Experiments have shown that the reading of the electrical resistance strain gauge tends to decrease from an initial value if the specimen surface is subjected to a suddenly large load. The creep effect is caused by the partial debonding of the glue that bonds the gauge to the surface, which results in measurement error[12].

2.2.3 Vibrating wire strain gauge

The vibrating wire strain gauge operates on the principle that the natural frequency of a pretensioned wire is affected by the stress applied to it. The relationship between the natural frequency f and the stress σ .

$$f = \frac{1}{2l} \sqrt{\frac{\sigma}{\rho}} \quad (2.1)$$

where ρ is the wire material density and l the length of the wire.

The vibrating wire gauge is very simple in design. Two anchors are installed on the specimen surface and the two ends of the wire are attached to the anchors. Once the stress σ of the wire is known using Equation 2.1, the strain of the surface can be found too, assuming the wire deformation faithfully follows the surface deformation. The advantage of the wire vibration gauge is that the gauge (wire) can be removed from the specimen, which makes it a suitable tool for long-term monitoring of strain change in the concrete structure. The major drawback of the wire vibration gauge is its sensitivity to ambient temperature. It is reported that a 1-degree temperature change causes a $20\mu\epsilon$ change in the strain measurement[13]. In some situations, the specimen temperature changes rapidly, either due to ambient temperature change, or due to active heating to the concrete mix to expedite the cure process. Unless the thermal expansion factor of the specimen is the same of that of the wire, measurement error is introduced. It is possible

to compensate the error caused by the temperature change, but doing so greatly complicates the system. Figure below shows the vibrating wire strain gauge.

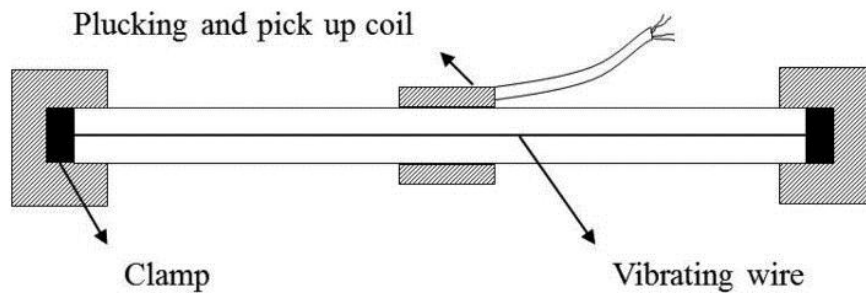


Figure 2.4: Vibrating wire strain gauge[14]

2.2.4 Video extensometer

A video extensometer measures the surface strain by tracking the coordinates of contrasting marks placed on the specimen. The gauge marks can be in the form of grid of dots or lines as shown in Figure 2.5, with the dot diameter or line thickness ranging from half millimeter to a couple of millimeters. The video image captured by the digital camera is analyzed by the image processing algorithms to locate the centers of the dots or the edges of the lines. During the test, the centers of the dots or the edges of the lines are followed automatically by the software. Their coordinate changes are used to extract the specimen strain information[15].

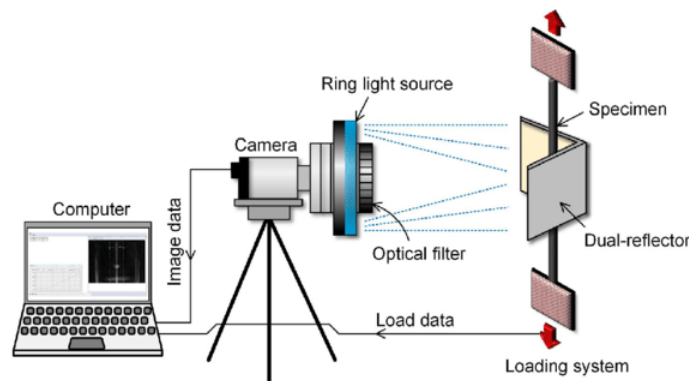


Figure 2.5: Video extensometer configuration[16]

Since the surface strain is measured by tracking a center of the mark, fine marks must be applied to the surface, such as a 7x7 grid of 0.5 mm diameter dots as described in wood surface strain measurement. For a material with irregular or soft surface, the application of marks may not be practical.

Some other Video extensometers, such as the MTS LX Laser Extensometer, use tapes instead of marks to tag the surface displacement. The tape that attaches to the specimen surface has strip spacing on it. The extensometer determines the surface strain by measuring the extension of the strip spacing. The technique is not a real noncontact measurement method since the tape contacts the specimen surface. It is possible that the strip and the specimen extend or shrink by different amounts due to a creep effect, so that the strain measured from the tape does not faithfully represent the actual specimen strain. The resolution is limited by tape strip spacing and usually low[17].

2.2.5 Laser speckle strain measurement

Speckle is generated by illuminating a rough surface with coherent light as shown in Figure 2.6. The random reflected waves interfere with each other, resulting in a grainy image, as shown Figure 2.7. The speckle pattern could be thought of as a “fingerprint” of the illuminated area, in the sense that the speckle pattern produced by every surface area is unique. Furthermore, when the surface area undergoes movement or deformation the speckle patterns in the image plane will also move or deform accordingly.

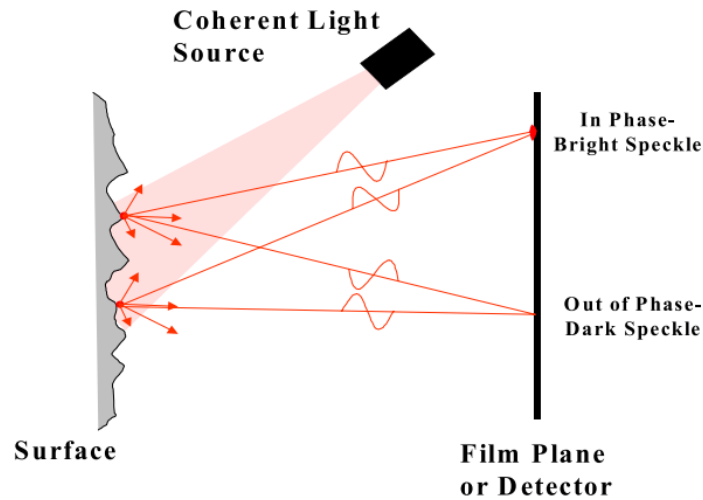


Figure 2.6: Principle of speckle generation[18]

There exist two basic categories of speckle technique for surface strain measurement: electronic speckle pattern interferometry (ESPI) and digital speckle photography (DSP). They relate to different methods of producing and processing the speckle image. The ESPI technique measures the object surface displacement or deformation by detecting the corresponding phase change of the light wave from reflected from the surface, just as a conventional Michelson interferometer does. The image taken in an ESPI system, called a “speckle interferogram”, is produced by interfering the speckle radiation reflected from an object surface with a reference light field, either a uniform coherent light beam or another speckle field[19]. In practice, the speckle interferograms are taken both before and after the object displacement or deformation.

REFERENCE

- [1] H. Fu, "Polarization-maintaining photonic crystal fiber based sensors and fiber Bragg gratings sensor system." The Hong Kong Polytechnic University, 2009.
- [2] A. Majumdar, "Development Of Optical Fiber Sensors For Distance, Refractive Index And Strain Measurement," 2009.
- [3] N. A. ALjaber and G. O. AL-Hassnawy, "Designing and Constructing the Strain Sensor Using Microbend Multimode Fiber," *Baghdad Sci. J.*, vol. 15, no. 2, pp. 217–220, 2018.
- [4] R. Li, Y. Tan, Y. Chen, L. Hong, and Z. Zhou, "Investigation of sensitivity enhancing and temperature compensation for fiber Bragg grating (FBG)-based strain sensor," *Opt. Fiber Technol.*, vol. 48, pp. 199–206, 2019.
- [5] M. S. Avila-Garcia *et al.*, "High sensitivity strain sensors based on single-mode-fiber core-offset Mach-Zehnder interferometers," *Opt. Lasers Eng.*, vol. 107, pp. 202–206, 2018.
- [6] P. Jia *et al.*, "'Bellows spring-shaped' ultrasensitive fiber-optic Fabry-Perot interferometric strain sensor," *Sensors Actuators A Phys.*, vol. 277, pp. 85–91, 2018.
- [7] H. Gong, C. C. Chan, L. Chen, and X. Dong, "Strain sensor realized by using low-birefringence photonic-crystal-fiber-based Sagnac loop," *IEEE Photonics Technol. Lett.*, vol. 22, no. 16, pp. 1238–1240, 2010.
- [8] W. Zhao, "Development of a portable optical strain sensor with applications to diagnostic testing of prestressed concrete." Kansas State University, 2011.
- [9] W. Zhao, B. T. Beck, R. J. Peterman, R. Murphy, C.-H. J. Wu, and G. Lee, "A direct comparison of the traditional method and a new approach in determining 220 transfer lengths in prestressed concrete railroad ties," in *2013 Joint Rail Conference*, 2013, p. V001T01A012-V001T01A012.

- [10] M. A. Muspratt, "STRAIN MEASUREMENT IN REINFORCED CONCRETE SLABS," *Strain*, vol. 5, no. 3, pp. 152–156, 1969.
- [11] A. L. Window, *Strain gauge technology*. Springer, 1992.
- [12] M. E. Tuttle and H. F. Brinson, "Resistance-foil strain-gage technology as applied to composite materials," *Exp. Mech.*, vol. 24, no. 1, pp. 54–65, 1984.
- [13] S. A. Neild, M. S. Williams, and P. D. McFadden, "Development of a vibrating wire strain gauge for measuring small strains in concrete beams," *Strain*, vol. 41, no. 1, pp. 3–9, 2005.
- [14] S. Choi, Y. Kim, J. Kim, and H. Park, "Field monitoring of column shortenings in a high-rise building during construction," *Sensors*, vol. 13, no. 11, pp. 14321–14338, 2013.
- [15] K. B. Dahl and K. A. Malo, "Planar strain measurements on wood specimens," *Exp. Mech.*, vol. 49, no. 4, pp. 575–586, 2009.
- [16] B. Dong, L. Tian, and B. Pan, "Tensile testing of carbon fiber multifilament using an advanced video extensometer assisted by dual-reflector imaging," *Measurement*, vol. 138, pp. 325–331, 2019.
- [17] MTS Systems Corporation, "The LX Laser Extensometer Series," 2009. [Online]. Available: http://www.mts.com/cs/groups/public/documents/library/dev_003699.pdf.
- [18] W. Zhao, R. L. Murphy, R. J. Peterman, B. T. Beck, C.-H. John Wu, and P. N. Duong, "Noncontact inspection method to determine the transfer length in pretensioned concrete railroad ties," *J. Eng. Mech.*, vol. 139, no. 3, pp. 256–263, 2012.
- [19] J. C. Dainty, *Laser speckle and related phenomena*, vol. 9. Springer science & business Media, 2013.
- [20] E. Udd and W. B. Spillman Jr, *Fiber optic sensors: an introduction for engineers and scientists*. John Wiley & Sons, 2011.

- [21] W. Gornall and T. Amarel, "Applications and techniques for fiber Bragg grating sensor measurements," *EXFO Burelgh Prod. Gr. Inc., New York*, 2003.
- [22] M. Sugiyama, "Tunable laser source." Google Patents, 07-Dec-2017.
- [23] I.-K. Yun, J. Lee, S.-W. Kim, and S. Hwang, "Broadband light source." Google Patents, 26-Jun-2007.
- [24] M. Nikles, L. Thévenaz, and P. A. Robert, "Simple distributed fiber sensor based on Brillouin gain spectrum analysis," *Opt. Lett.*, vol. 21, no. 10, pp. 758–760, 1996.
- [25] A. G. Simpson, K. Zhou, L. Zhang, L. Everall, and I. Bennion, "Optical sensor interrogation with a blazed fiber Bragg grating and a charge-coupled device linear array," *Appl. Opt.*, vol. 43, no. 1, pp. 33–40, 2004.
- [26] T. G. Giallorenzi *et al.*, "Optical fiber sensor technology," *IEEE Trans. Microw. Theory Tech.*, vol. 30, no. 4, pp. 472–511, 1982.
- [27] J. W. Berthold, "Historical review of microbend fiber-optic sensors," *J. Light. Technol.*, vol. 13, no. 7, pp. 1193–1199, 1995.
- [28] Vangal, "optical fiber types," 2009. [Online]. Available: <https://www.classle.net/#!/classle/book/optical-fiber-types/>.
- [29] H. S. Efendioglu, T. Yildirim, and K. Fidanboyu, "Prediction of force measurements of a microbend sensor based on an artificial neural network," *Sensors*, vol. 9, no. 9, pp. 7167–7176, 2009.
- [30] B. Peeters, F. L. M. dos Santos, A. Pereira, and F. Araujo, "On the use of optical fiber Bragg grating (FBG) sensor technology for strain modal analysis," in *AIP conference proceedings*, 2014, vol. 1600, no. 1, pp. 39–49.
- [31] A. Othonos, "Bragg gratings in optical fibers: fundamentals and applications," in *Optical Fiber Sensor Technology*, Springer, 2000, pp. 79–187.
- [32] S. W. James, M. L. Dockney, and R. P. Tatam, "Simultaneous independent temperature and strain measurement using in-fibre Bragg grating sensors,"

Electron. Lett., vol. 32, no. 12, pp. 1133–1134, 1996.

- [33] D. Yuan, Y. Dong, Y. Liu, and T. Li, “Mach-zehnder interferometer biochemical sensor based on silicon-on-insulator rib waveguide with large cross section,” *Sensors*, vol. 15, no. 9, pp. 21500–21517, 2015.
- [34] B. H. Lee *et al.*, “Interferometric fiber optic sensors,” *Sensors*, vol. 12, no. 3, pp. 2467–2486, 2012.
- [35] H. Y. Choi, K. S. Park, S. J. Park, U.-C. Paek, B. H. Lee, and E. S. Choi, “Miniature fiber-optic high temperature sensor based on a hybrid structured Fabry–Perot interferometer,” *Opt. Lett.*, vol. 33, no. 21, pp. 2455–2457, 2008.
- [36] F. L. S. J. Pedrotti, L. S. Pedrotti, and L. M. Pedrotti, “Introduction to optics,” 2007.
- [37] W.-H. Tsai and C.-J. Lin, “A novel structure for the intrinsic Fabry-Perot fiber-optic temperature sensor,” *J. Light. Technol.*, vol. 19, no. 5, pp. 682–686, 2001.
- [38] Y.-J. Rao, “Recent progress in fiber-optic extrinsic Fabry–Perot interferometric sensors,” *Opt. Fiber Technol.*, vol. 12, no. 3, pp. 227–237, 2006.
- [39] K. P. Koo, M. LeBlanc, T. E. Tsai, and S. T. Vohra, “Fiber-chirped grating Fabry-Perot sensor with multiple-wavelength-addressable free-spectral ranges,” *IEEE photonics Technol. Lett.*, vol. 10, no. 7, pp. 1006–1008, 1998.
- [40] Y. X. Ng, A. I. Azmi, M. Y. M. Noor, A. S. Abdullah, and R. K. R. Ibrahim, “Investigation of Michelson Interferometer Fiber Temperature Sensor Based on Single Mode-Multimode-Single Mode Fiber Structure,” *Elektr. Electr. Eng.*, vol. 16, no. 3, pp. 6–10, 2017.
- [41] D. Zazula, D. Donlagić, and Š. Sprager, “Unobtrusive monitoring of biomedical signals in home environment,” in *Telecommunications Forum (TELFOR), 2011 19th*, 2011, pp. 31–34.
- [42] Y. Yang, L. Lu, F. Yang, Y. Chen, and W. Jin, “The fiber optic Sagnac interferometer and its sensing application,” in *2015 Optoelectronics Global*

Conference (OGC), 2015, pp. 1–6.

- [43] S. Xiao *et al.*, “Simultaneous measurement of refractive index and temperature using SMP in Sagnac loop,” *Opt. Laser Technol.*, vol. 96, pp. 254–258, 2017.
- [44] Z. Yin *et al.*, “Fiber ring laser sensor for temperature measurement,” *J. Light. Technol.*, vol. 28, no. 23, pp. 3403–3408, 2010.
- [45] S. Xiao, B. Wu, Y. Dong, H. Xiao, S. Yao, and S. Jian, “Strain and temperature discrimination using two sections of PMF in Sagnac interferometer,” *Opt. Laser Technol.*, vol. 113, pp. 394–398, 2019.
- [46] Z. Liu, Z. Tan, B. Yin, Y. Bai, and S. Jian, “Refractive index sensing characterization of a singlemode–claddingless–singlemode fiber structure based fiber ring cavity laser,” *Opt. Express*, vol. 22, no. 5, pp. 5037–5042, 2014.
- [47] P. Zu *et al.*, “A temperature-insensitive twist sensor by using low-birefringence photonic-crystal-fiber-based Sagnac interferometer,” *IEEE Photonics Technol. Lett.*, vol. 23, no. 13, pp. 920–922, 2011.
- [48] H. Zhang, Y. Lu, L. Duan, Z. Zhao, W. Shi, and J. Yao, “Intracavity absorption multiplexed sensor network based on dense wavelength division multiplexing filter,” *Opt. Express*, vol. 22, no. 20, pp. 24545–24550, 2014.
- [49] S. Zhen, R. Liu, B. Yu, J. Zhang, and B. Han, “A fiber micro-vibration sensor based on single-mode fiber ring laser,” *Chinese Opt. Lett.*, vol. 7, no. 1, pp. 26–28, 2009.
- [50] S. Chowdhury, S. Verma, and T. K. Gangopadhyay, “A comparative study and experimental observations of optical fiber sagnac interferometric based strain sensor by using different fibers,” *Opt. Fiber Technol.*, vol. 48, pp. 283–288, 2019.
- [51] C. Shangguan, W. Zhang, W. Hei, F. Luo, and L. Zhu, “Fabry–Perot cavity cascaded sagnac loops for temperature and strain measurements,” *Opt. Eng.*, vol. 57, no. 4, p. 47103, 2018.
- [52] N. A. B. Ahmad, S. H. Dahlan, and N. A. Cholan, “Theoretical Analysis of a

- Two-stage Sagnac loop filter using Jones Matrices,” *Int. J. Electr. Comput. Eng.*, vol. 7, no. 6, pp. 2950–2957, 2017.
- [53] M. Zhou, Z. Luo, Z. Cai, C. Ye, H. Xu, and J. Wang, “Switchable and tunable multiple-channel erbium-doped fiber laser using graphene-polymer nanocomposite and asymmetric two-stage fiber Sagnac loop filter,” *Appl. Opt.*, vol. 50, no. 18, pp. 2940–2948, 2011.
- [54] O. J. Rashid, “Characterization of Polarization-maintaining Fibers,” 2015.
- [55] C. Shangguan, W. Zhang, W. Hei, F. Luo, and L. Zhu, Fabry–Perot cavity cascaded sagnac loops for temperature and strain measurements, *Opt. Eng.*, vol. 57, no. 4, p. 47103, 2018.
- [56] G. Sun, Y. Cen, L. Zhao, C. Wei, and Y. Chung, “Combined Sagnac and intermodal interferences for discrimination of strain and temperature variations,” in *2017 25th Optical Fiber Sensors Conference (OFS)*, 2017, pp. 1–4.
- [57] G. H. Kim, S. M. Park, C. H. Park, H. Jang, C.-S. Kim, and H. D. Lee, “Real-time quasi-distributed fiber optic sensor based on resonance frequency mapping,” *Sci. Rep.*, vol. 9, no. 1, p. 3921, 2019.
- [58] L. Meng, L. Wang, and Y. Hou, “Development of Large-Strain Macrobend Optical-Fiber Sensor with Helical-Bending Structure for Pavement Monitoring Application,” *J. Aerosp. Eng.*, vol. 32, no. 3, p. 4019021, 2019.
- [59] S. Xiao, B. Wu, Y. Dong, H. Xiao, S. Yao, and S. Jian, “Strain and temperature discrimination using two sections of PMF in Sagnac interferometer,” *Opt. Laser Technol.*, vol. 113, pp. 394–398, 2019.
- [60] Y. Kim, S. Ju, S. Jeong, S. H. Lee, Y. Kim, and W.-T. Han, “Effect of F doping in the core of a birefringent photonic crystal fiber on sensing capability of temperature and strain sensors,” in *2017 25th Optical Fiber Sensors Conference (OFS)*, 2017, pp. 1–4